Supporting information

Critical Role of Interfacial Diffusion and Diffuse Interphases Formed in Multi Micro-/Nanolayered Polymer Films Based on Poly(Vinylidene Fluoride) and Poly(Methyl Methacrylate)

Bo Lu,[†] *Khalid Lamnawar,*[*,†] *Abderrahim Maazouz,*[†,§] *and Guillaume Sudre*[‡]

[†] Université de Lyon, CNRS, UMR 5223, Ingénierie des Matériaux Polymères, INSA Lyon, F-69621,Villeurbanne, France

[‡] Université de Lyon, CNRS, UMR 5223, Ingénierie des Matériaux Polymères, Université Claude Bernard Lyon 1, F-69622, Villeurbanne, France

[§] Hassan II Academy of Science and Technology, 10100 Rabat, Morocco

[*] Corresponding author: khalid.lamnawar@insa.lyon.fr (K. L.)

1. Linear viscoelasticity of the investigated neat polymers

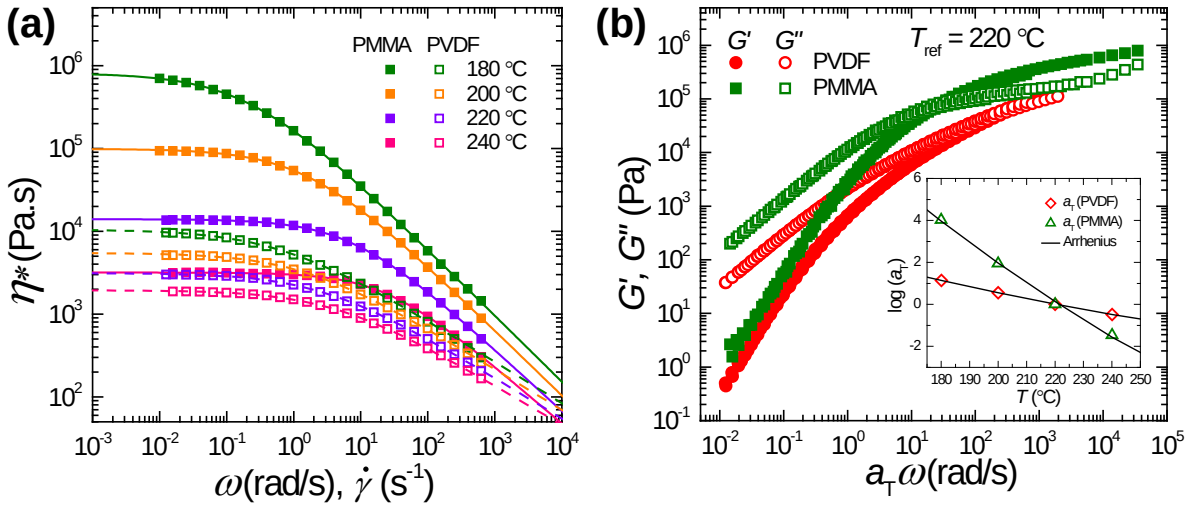

Figure S1. (a) Complex viscosity versus angular frequency (shear rate) for neat polymers at different temperatures. Lines in (a) are fits to the Carreau-Yasuda model. (b) Master curves of storage modulus (G') and loss modulus (G'') reduced at a reference temperature of 220 °C for PVDF and PMMA. The inset in (b) shows the shift factors (a_T) *versus* temperature. Lines in the inset are fits to Arrhenius equation.

Linear viscoelastic properties of neat polymers were determined by small-amplitude oscillatory shear (SAOS) measurements at temperatures ranging from 180 to 220 ^{o}C. Figure S1a plots the dynamic complex viscosity (η^*) against angular frequency (ω) for neat polymers at temperatures between 180 and 220 ^{o}C, which could be also taken as the scenario of steady-state shear viscosity (η) plotted against shear rate ($\dot{\gamma}$) according to the Cox-Merz rule:[1]

$$\eta(\dot{\gamma}) = \left|\eta^*(\omega)\right|_{\dot{\gamma}=\omega} \tag{1}$$

The zero-shear viscosity (η_0) was estimated by fitting the data transformed from oscillatory data by Eq. (1) to the Carreau-Yasuda model:[2]

$$\frac{\eta(\dot{\gamma}) - \eta_\infty}{\eta_0 - \eta_\infty} = \left[1 + (\lambda\dot{\gamma})^a\right]^{\frac{n-1}{a}} \tag{2}$$

where η_∞ is the infinite-shear-rate viscosity, λ is the a characteristic viscous relaxation time that defines the location of the transition from Newtonian to shear-thinning behaviour ($1/\lambda$ is the critical shear rate at the onset of shear thinning). a is a dimensionless parameter (sometimes called "the Yasuda constant" since it was a parameter added to the Carreau equation by Yasuda) which describes the transition zone between the Newtonian plateau and the shear-thinning region and is inversely related to the breadth of this zone.[2] The exponent (n - 1) defines the slope of the $\eta(\dot{\gamma})$ *versus* $\dot{\gamma}$ curve within the power law region. The fits of

the Carreau-Yasuda model are presented in Figure S1a (see lines). As shown in Figure S1a, both polymers display the shear-thinning behavior at higher frequencies and a Newtonian behavior at lower frequencies. PMMA exhibits a more pronounced shear-thinning behavior than PVDF at measured temperatures. Moreover, the turning point between these two regions moved toward higher frequencies when the temperature increased. It is worth mentioning that PMMA is more viscous than PVDF at the same temperature, but as the temperature is raised, their viscosities approach each other.

Table S1. Material characteristics based on linear viscoelastic measurements at 220 °C

Polymer	η_0 (Pa.s)	G_N^0 (Pa)	M_e (kg/mol)	Z=M_w/M_e	τ_{rep} (s)	τ_R (s)
PVDF	3.13×10^3	6.24×10^5	9.57	21.94	0.37	2.67×10^{-3}
PMMA	1.40×10^4	4.81×10^5	9.22	10.85	0.56	3.31×10^{-3}

Master curves of storage modulus (G') and loss modulus (G'') reduced at a reference temperaure of 220 ^{o}C with a time-temperature shift factor (a_T) are given in Figure S1b. The rheology at terminal zone is observed to keep the typical relations $G' \sim \omega^2$, $G'' \sim \omega$ for the neat polymers. The temperature dependence of the linear rheological behaviour follows the Arrhenius equation. Molecular characteristics based on linear viscoelastic measurements are listed in Table S1. Herein, zero-shear viscosity (η_0) was estimated with the Carreau-Yasuda model.[2] Plateau modulus (G_N^0) was determined with a semi-quantitative method based on the crossover modulus, as addressed in our earlier work.[3] Entanglement molecular weight (M_e) was calculated according to $G_N^0=\rho RT/M_e$ with the melt mass density (ρ) and gas constant (R). The number of entanglements per chain (Z) can be evaluated as $Z=M_w/M_e$. The weight average terminal relaxation time determined from the cole-cole plots ($\eta''\sim\eta'$) was taken as the order of reptation time (τ_{rep}). Furthermore, the Rouse relaxation time (τ_R) could be estimated according to the equation:[2, 4]

$$\tau_R = \frac{6M_w\eta_0}{\pi^2\rho RT}\left(\frac{M_c}{M_w}\right)^{2.4} \quad (3)$$

with taking the critical molecular weight M_c to be twice M_e.

2. Thermal stability of the investigated polymers

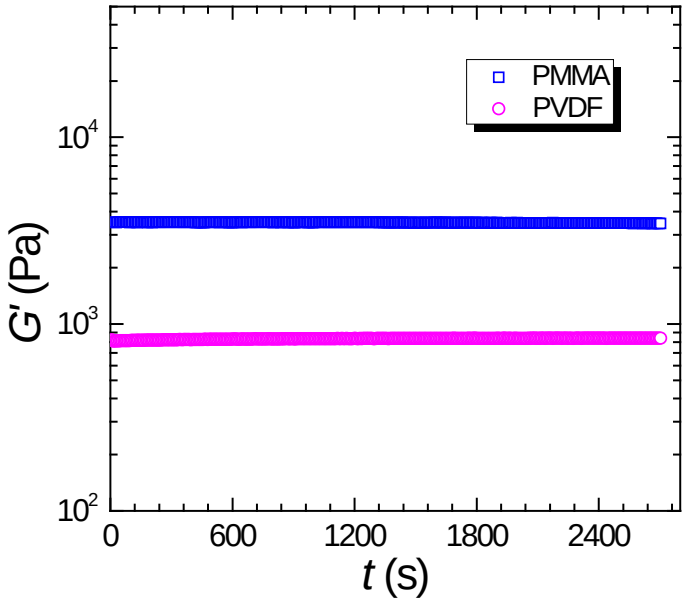

Figure S2. Storage modulus (G') as a function of time within 50 min for neat PVDF and PMMA measured at a given frequency of 1.0 rad/s, a strain amplitude of 1.0% and a temperature of 220 °C.

Prior to processing by multilayer coextrusion and probing the diffusion process of polymer bilayers in the molten state by rheology, it is indispensable to examine the thermal stability of the neat polymers under investigation at the processing and measured temperatures. Hence, dynamic time sweep tests for the neat polymers were conducted in advance under the same conditions as for the bilayer systems. Figure S2 shows the time evolution of storage modulus (G') within a period of 45 min for neat PVDF and PMMA measured at 220 °C with a given angular frequency of 1.0 rad/s and strain amplitude of 1.0%. The invariable change of the rheological responses with time, as clearly depicted in Figure S2, sufficiently indicates the thermal stability of these investigated polymers at the employed conditions.

3. WAXS/SAXS patterns for coextruded control films

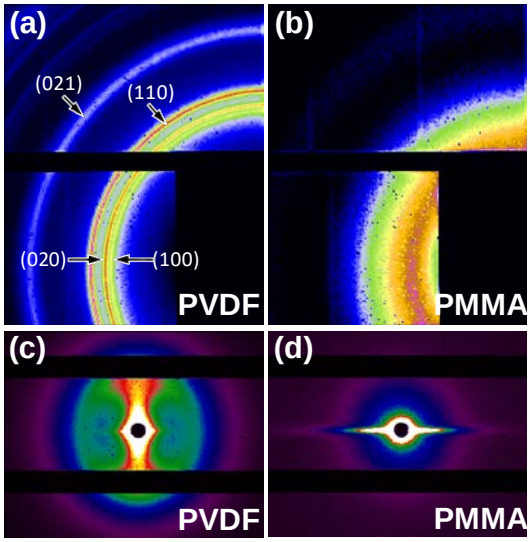

Figure S3. 2D-WAXS (a,b) and SAXS (c,d) patterns recorded with X-ray beam parallel to the extrusion direction (ED) for neat polymer control films: (a,c) PVDF, (b,d) PMMA.

4. DSC thermographs for multilayer films

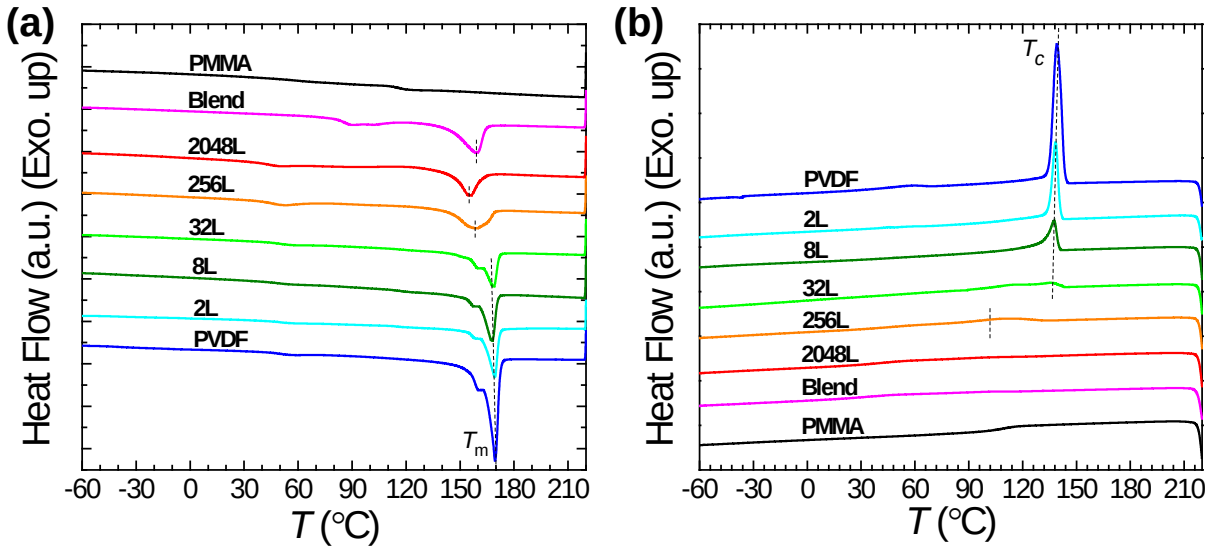

Figure S4. DSC thermographs of heating scan (a) and cooling scan (b) for PVDF/PMMA multilayer films, neat polymer control films and blend (50/50).

Figure S4 presents the DSC thermographs corresponding to the first heating (Figure S4a) and the subsequent cooling scan (Figure S4b) for PVDF/PMMA multilayers, blend (50/50) and neat polymers. As for microlayers with nominal layer thickness in the microscale (2L to 32L), the peak positions of endothermic melting peaks remain close to that of neat PVDF and negligibly move with increasing the number of layers (Figure S4a), despite the half peak area of the latter due to the 50% fraction in the multilayered systems. This suggests that PVDF crystallization in microlayered films is negligibly affected and behaves as bulk PVDF. However, the peak is obviously shifted towards lower temperatures for nanolayered films

(256L and 2048L), which signifies that the average of lamellar thickness decreases. Meanwhile, a broader peak (larger full width at half maximum, FWHM) can be also observed for nanolayered films, suggesting the wider distributions of spherulite size and lamellar thicknesses. Herein, average crystalline lamellar thickness (L_c) was calculated from the melting temperature (T_m) in the first DSC heating scan through the Gibbs-Thomson (G-T) equation:

$$T_m = T_m^0\left(1-\frac{2\sigma_e}{\Delta H_m^0}\frac{1}{L_c}\right) \quad (4)$$

where T_m^0 is the melting temperature of infinitely thick PVDF crystal, 483.2K;[5] and ΔH_m^0 is the melting enthalpy per unit volume of the PVDF crystal, 104.6 J/g;[6] σ_e is the surface free energy of the PVDF α-crystals, 38.0 dyn/cm.[7] Besides, the crystallinity in the multilayered films was derived from the first DSC heating scan according to:

$$X_c = \frac{\Delta H_m}{w\Delta H_m^0}\times 100\% \quad (5)$$

in which ΔH_m is the experimental enthalpy of fusion, w is the weight content of PVDF.

5. Dielectric relaxation spectra of neat polymers

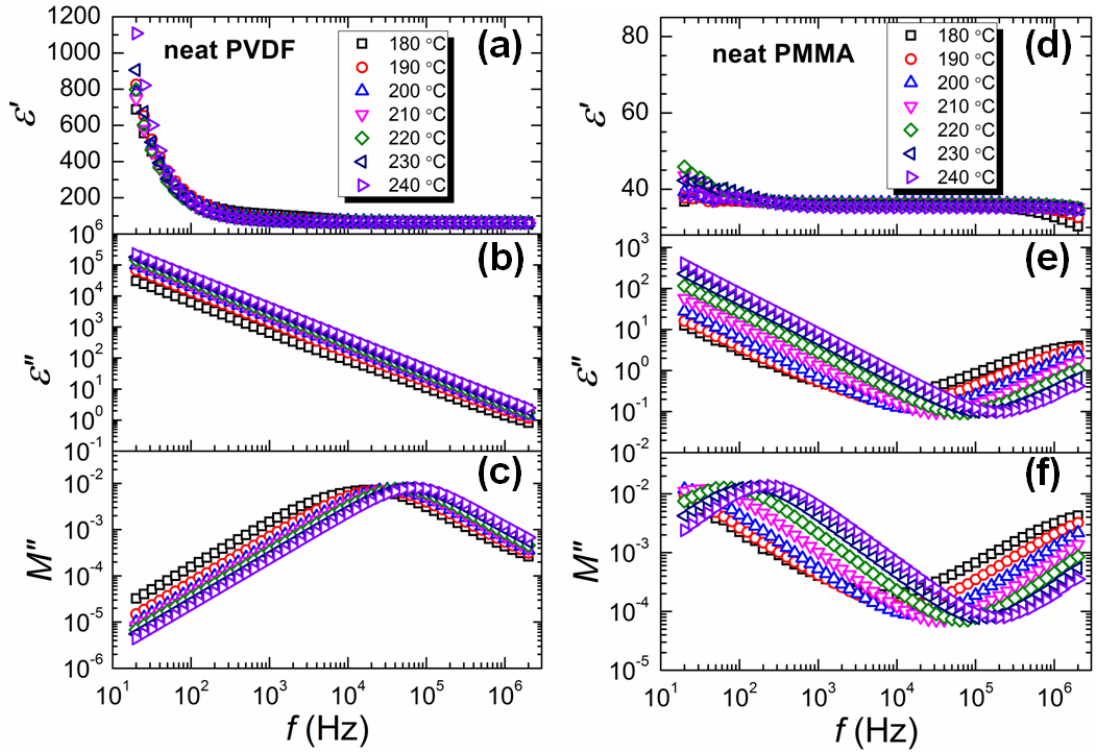

Figure S5. Different representations of the dielectric spectra recorded at temperatures ranging from 180 to 240 °C (10 °C increment) for (a)–(c) neat PVDF, and (d)-(f) neat PMMA.

References for Supporting Information:

[1] Cox, W. P.; Merz, E. H. Correlation of Dynamic and Steady Flow Viscosities, *J. Polym. Sci.* **1958,** *28*, (118), 619-622.

[2] Yasuda, K.; Armstrong, R.; Cohen, R. Shear Flow Properties of Concentrated Solutions of Linear and Star Branched Polystyrenes, *Rheol. Acta* **1981,** *20*, (2), 163-178.

[3] Lu, B.; Lamnawar, K.; Maazouz, A.; Zhang, H. Revealing the Dynamic Heterogeneity of PMMA/PVDF blends: from Microscopic Dynamics to Macroscopic Properties, *Soft Matter* **2016,** *12*, (13), 3252-3264.

[4] Dealy, J. M.; Larson, R. G., *Structure and Rheology of Molten Polymers*. Hanser Gardner Publications: Cincinnati, 2006.

[5] Nakagawa, K.; Ishida, Y. Annealing Effects in Poly(vinylidene fluoride) as Revealed by Specific Volume Measurements, Differential Scanning Calorimetry, and Electron Microscopy, *J. Polym. Sci., Part B: Polym. Phys.* **1973,** *11*, (11), 2153-2171.

[6] Teyssedre, G.; Bernes, A.; Lacabanne, C. Influence of the Crystalline Phase on the Molecular Mobility of PVDF, *J. Polym. Sci., Part B: Polym. Phys.* **1993,** *31*, (13), 2027-2034.

[7] Patki, R.; Mezghani, K.; Phillips, P. J., Crystallization Kinetics of Polymers. In *Physical Properties of Polymers Handbook*, Mark, J. E., Ed. Springer: New York, 2007; pp 625-640.